M. Amara[1], O. Bouledroua[2,3], M. Hadj Meliani[2,5], B.G.N. Muthanna[4], M. Tahar Abbes[1], G. Pluvinage[5]

ASSESSMENT OF PIPE FOR CO_2 TRANSPORTATION USING A CONSTRAINT MODIFIED CTOD FAILURE ASSESSMENT DIAGRAM

OCENA INTEGRITETA CEVI ZA TRANSPORT CO_2 PRIMENOM DIJAGRAMA OCENE LOMA SA OGRANIČENJEM MODIFIKOVANOG CTOD

Originalni naučni rad / Original scientific paper
UDK /UDC: 620.1:669.14
621.791.05:669.14
Rad primljen / Paper received: 5.09.2018

Adresa autora / Author's address:
[1)] Laboratory of Mechanics and Energetics, University Hassiba Benbouali of Chlef, Chlef, Algeria
[2)] LPTPM, Hassiba Ben Bouali University of Chlef, Chlef, Algeria, email: o.bouledroua@univhb-chlef.dz
[3)] Sonatrach/Division Technologies et Innovation, Boumerdès, Algeria
[4)] LRM, Hassib Ben Bouali University of Chlef, Chlef, Algeria
[5)] LE3M, University of Lorraine, Metz, France

Keywords
- FAD
- T stress
- pipe defect
- safety factor

Abstract

Failure Assessment Diagram (FAD) is constraint modified using the assumption that the constraint T stress is proportional to the non-dimensional loading. The constraint modified FAD has been used to compute safety factors associated elliptic defects.

Ključne reči
- FAD
- T napon
- greške u cevima
- stepen sigurnosti

Izvod

Uvedena je modifikacija ograničenjem dijagrama ocene loma (FAD), pod pretpostavkom da su ograničavajući T naponi proporcionalni bezdimenzionom opterećenju. Modifikovani FAD je upotrebljen kako bi se izračunali faktori sigurnost vezani za eliptičke greške.

FRACTURE TOUGHNESS AND CONSTRAINT

Critical CTOD is a measure of fracture toughness /1/. As other measures of fracture toughness, critical CTOD is sensitive to ligament size, loading mode and thickness. Han et al. /2/ have shown that the critical CTOD of a pipe steel API 5L X65 decreases when the thickness increases and reaches an asymptotic value for specimen of 18 mm thickness. The effect of constraint is attributed to one of the following parameters: the plastic constraint factor L, the stress triaxiality β, the Q parameter, T stress, and A_2 /3/. In this case the authors use the stress triaxiality defined as the ratio of the hydrostatic stress over the equivalent von Misses stress,

$$\beta = \frac{\sigma_h}{\sigma_{VM}}, \tag{1}$$

where:
$$\sigma_k = \frac{\sigma_{xx} + \sigma_{yy} + \sigma_{zz}}{3}, \tag{2}$$

and:
$$\sigma_{VM} = \frac{1}{\sqrt{2}}\sqrt{(\sigma_1 - \sigma_3)^2 + (\sigma_1 - \sigma_2)^2 + (\sigma_2 - \sigma_3)^2}\ . \tag{3}$$

The critical stress triaxiality distribution at the crack tip increases until it reaches a maximum, which for the critical event is called $\beta_{max,c}$ and corresponds to the distance $X_{\beta max,c}$. Afterwards, it decreases, then sometimes increases again, and finally falls to zero when the distance is far from the crack tip.

Evolution of the critical CTOD versus the stress triaxiality β is presented in Fig. 1 for the API 5L X 65 pipe steel. Parameter δ_c decreases linearly with b and reaches an asymptotic value for $\beta^* = 2.5$.according to:

$$\delta_c = \delta_{c,0} + \alpha\beta\,, \tag{4}$$

where: δ_c is the reference CTOD for high constraint ($\beta > 2.5$); and α is a constant.

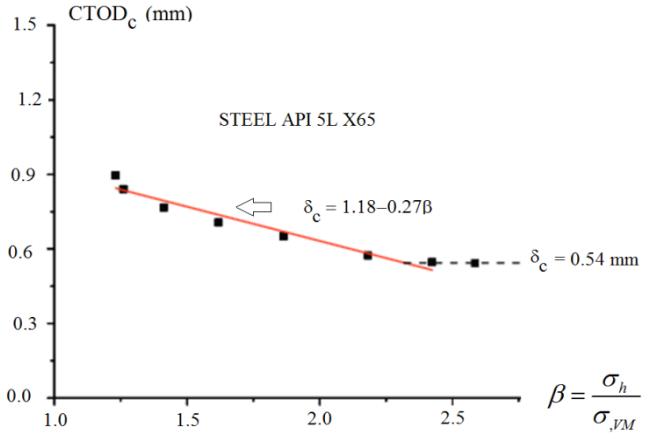

Figure 1. Evolution of critical CTOD versus the stress triaxiality β for API 5L X 65 pipe steel, /2/.

NUMERICAL ANALYSIS

A finite element code called Ansys APDL has been used to model the pipe geometry Fig. 2(a), according to the symmetry we have illustrated only a half of the pipe. A SOLID186 element used in this finite element analysis with 16 node quadrilateral elements has been adapted to meshing the pipe, and we have refined the mesh near the crack tip which represents the critical zone of the pipe, Fig. 2(a). The

pipe of diameter D = 219 mm and thickness t = 6.1 mm, the semi-elliptical crack dimensions are presented in Fig. 2(c) with a as the crack depth, and c as the crack length. An example is shown of opening stress distribution at the semi-elliptical crack tip for P = 20.1 MPa and a/t =0.5 and a/c = 0.2.

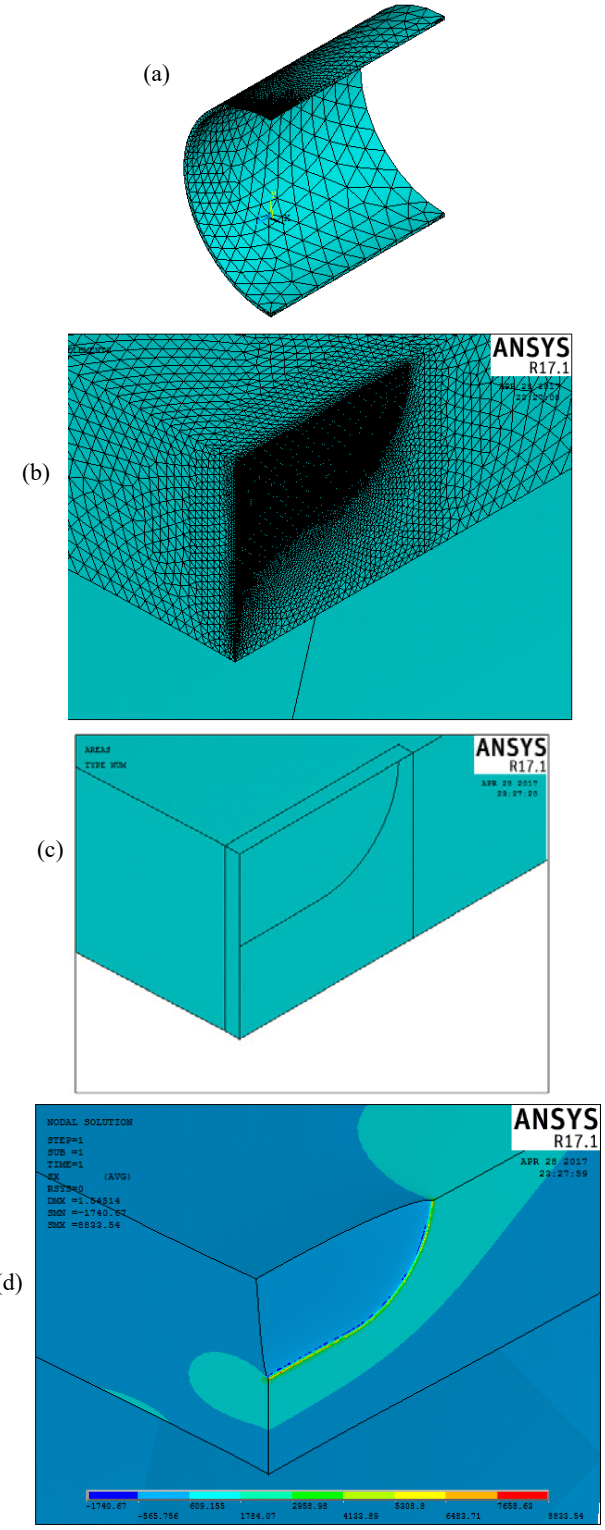

Figure 2. Semi-elliptical crack in pipeline with a/t = 0.5 and a/c = 0.2. (a) Pipeline geometry and meshing, (b) meshing type, (c) crack dimension, (d) opening stress distribution at crack tip.

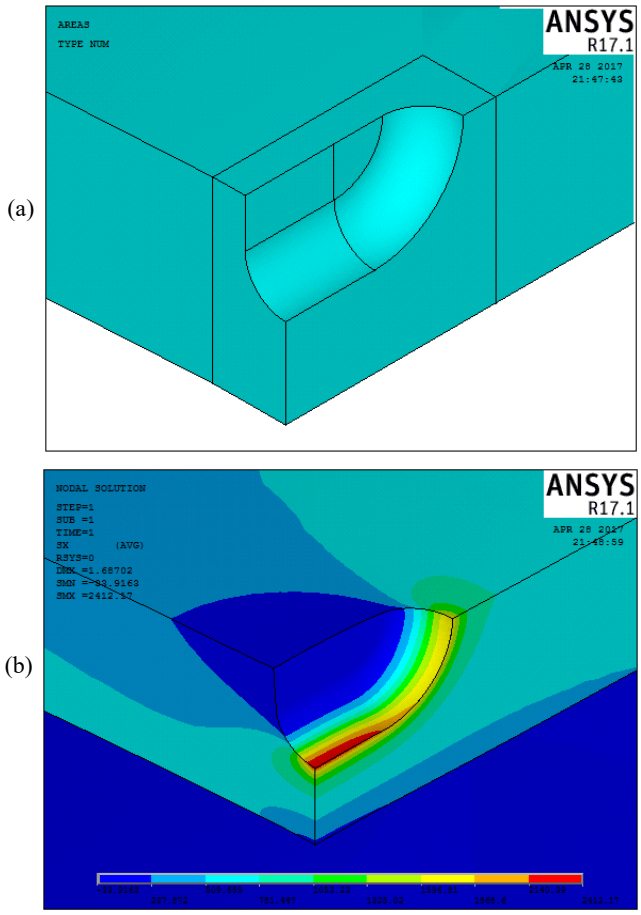

Figure 3. Semi-elliptical defect at pipeline with a/t = 0.5, a/c = 0.2 and ρ = 2.5 mm. (a) Pipeline geometry, (b) opening stress distribution at defect tip.

In Fig. 3(a) a semi-elliptical defect geometry with notch radius is shown, and the opining stress distribution is presented in Fig. 3(b). The maximal stress is localized at the defect tip with a stress ratio between crack and notch of 3.66. In this work; we have studied the effect of pressure and crack radius on the triaxiality β. Firstly, we have studied the effect of loading pressure on triaxiality β. Non-dimensional stress L_r is described as the ratio of the gross stress σ_g over flow stress (chosen as yield stress σ_y, ultimate stress σ_u or classical flow stress P_L). The result of loading pressure effect is presented in Fig. 4. The applied pressure has no effect on the value of triaxiality β. It is submitted to internal pressure p until limit pressure P_L. The limit pressure is given by the ASME formulae, /4/:

$$P_L = \frac{2(1.1\sigma_y)t}{D} \times \left[\frac{1-(2/3)(a/t)}{1+0.8(2/3)(a/t)M} \right], \tag{5}$$

$$M = \sqrt{1+0.8\left(\frac{2c}{D}\right)^2 \left(\frac{D}{t}\right)}. \tag{6}$$

The value of the limit load is in this case P_L = 20.1 MPa. The triaxiality β has been computed assuming elastic behaviour for different L_r values.

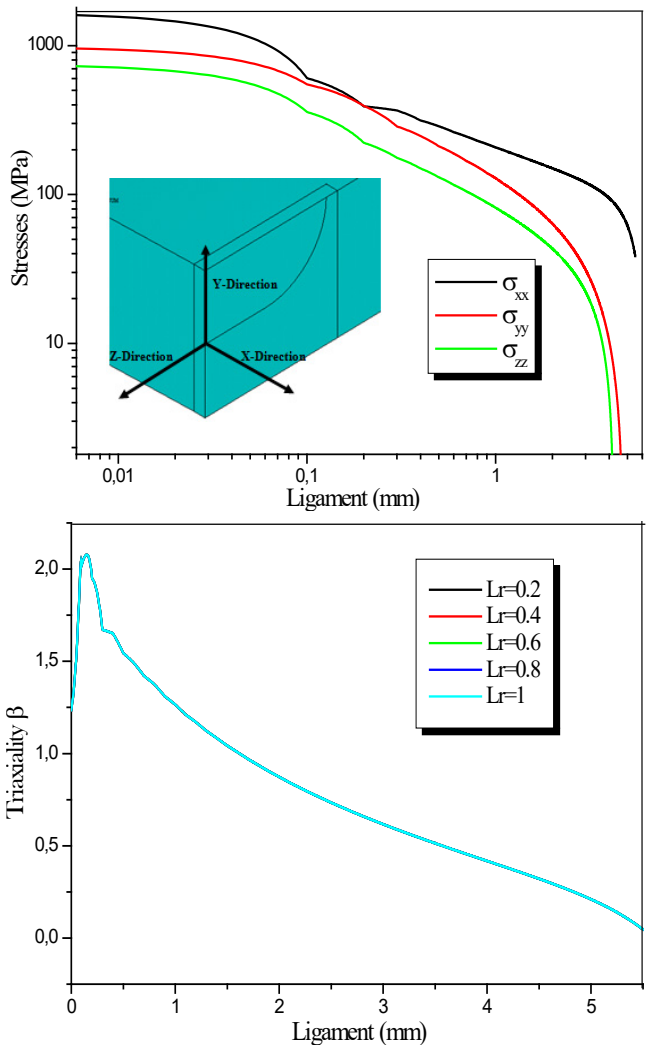

Figure 4. Stresses and triaxiality distribution at ligament of cracked pipeline with different pressure values.

In the second part; we have studied the effect of crack radius on triaxiality β, the crack length $a/t = 0.5$, the pressure $P = 20.1$ MPa, and the radius $\rho = 0$ to 2.5 mm. The results are presented in Fig. 5.

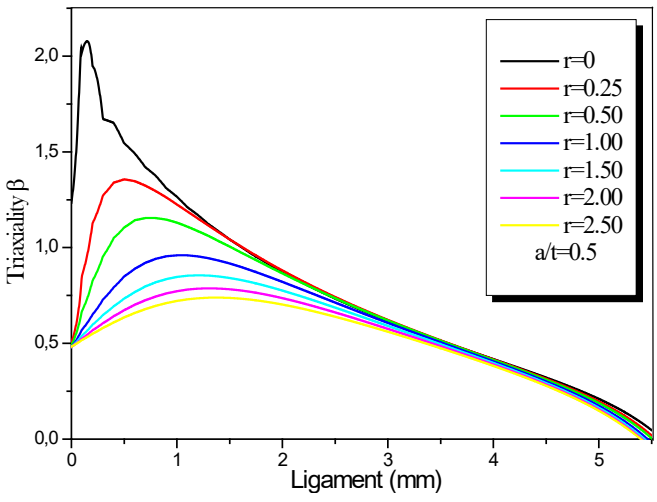

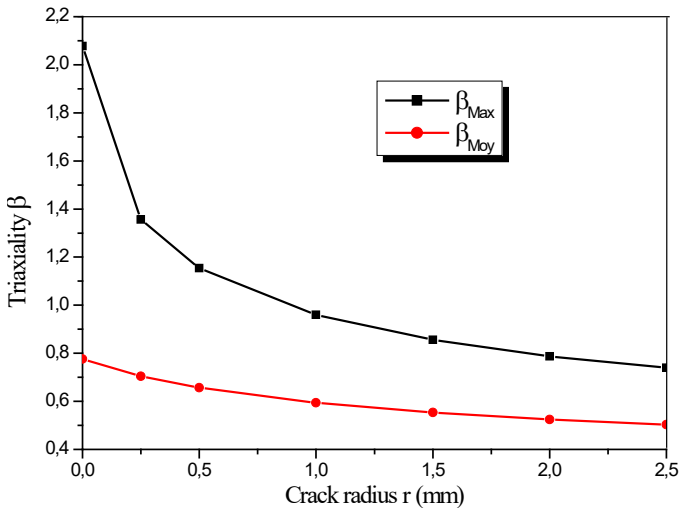

Figure 5. Crack radius effect on triaxiality β. (a) Triaxiality distribution at crack ligament, (b) maximal and medium value variation for $\rho = 0$ to 2.5 mm.

FAILURE ASSESSMENT DIAGRAM

The FAD methodology replaces three fracture mechanic parameters relationship (fracture toughness, defect size and loading) by two parameters, one in order to have a plane representation where non-dimensional crack driving force k_r and non-dimensional applied stress L_r are the coordinates. The non-dimensional crack driving force k_r is defined as the square root of the ratio of applied CTOD δ_{ap}, to the fracture toughness of the material δ_c,

$$k_r = \sqrt{\frac{\delta_{ap}}{\delta_c}}\,. \tag{7}$$

Non-dimensional stress L_r is described as the ratio of gross stress σ_g over flow stress (chosen as yield stress σ_Y, ultimate stress σ_U, or classical flow stress $\sigma_0 = (\sigma_y + \sigma_U)/2$,

$$L_r = \frac{\sigma_g}{\sigma_0} \quad \text{or} \quad L_r = \frac{P}{P_L}\,. \tag{8}$$

The failure assessment curve is obtained from fracture toughness data measured from specimens tested under high levels of constraint and with an unknown β value, but probably close to 2.5.

The modified constraint FAD /5/ is obtained by taking into account that the material fracture toughness is sensitive to constraint and therefore, the failure assessment curve is modified. Here, one assumes that the triaxiality is proportional to non-dimensional load:

$$\beta = \beta_\delta L_r\,. \tag{9}$$

In Fig. 1 and Eq.(9) $\alpha = -0.27$ and $\beta_\delta = 1$. Combining Eqs.(4) and (9), one gets:

$$\delta_c = \delta_{c,0}(1 + \alpha(\beta_\delta L_{r,c}))\,. \tag{10}$$

The failure curve for the basic level and for the reference fracture toughness ($\beta = 2.5$) is given by Eq.(11):

$$f(L_r) = \frac{1}{\sqrt{1 + \frac{L_r^2}{2}}}\left[0.3 + 0.7\exp(-\mu L_r^6)\right] \quad \text{for} \quad 0 \le L_r \le L_{r,\max} \tag{11}$$

The failure assessment curve for any value of constraint is given as:

$$K_{r,c} = f(L_r)\sqrt{1+\alpha(\beta_{T\alpha}, L_{r,c})}\,. \tag{12}$$

The failure assessment curve is then modified according to Eq.(12) and compared to the reference failure assessment curve, called $f(L_r)_{\beta=2.5}$. Both curves are plotted in Fig. 6. The failure assessment curve $f(L_r)_{structr}$ lies above the reference curve. The maximal difference is obtained from $L_r = 0.7$ and is about 21%.

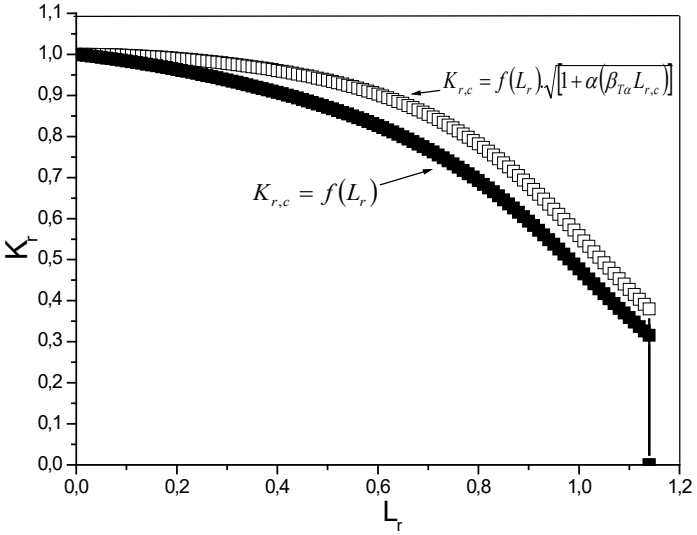

Figure 6. Failure assessment curves $f(L_r)_{\beta=2.5}$ and $f(L_r)_{struct}$.

SAFETY FACTOR DETERMINED BY MODIFIED FAD

The assessment point is defined by following coordinates:

$$k_r = \sqrt{\frac{\delta_{ap}}{\delta_c}}\,, \tag{13}$$

where: δ_{ap} is the applied notch stress intensity factor; and δ_c is the fracture toughness of the material.

In traditional approach, the fracture toughness is determined according to standard with a high constraint specimen. This value can be identified as $k_{mat} = k^0_{\rho,c}$. Therefore, a reference value of k_c^* is given by:

$$k^*_{c,ref} = \sqrt{\frac{\delta_{ap}}{\delta_c}}\,. \tag{14}$$

In order to reduce the conservatism induced by the use of the high constraint specimen, and taking into account the increase of fracture toughness by the loss of constraint, we define the coordinates of the assessment point devoted to a structure by:

$$k^*_{c,struct} = \sqrt{\frac{\delta_{ap}}{\delta_{c,0}}}\,. \tag{15}$$

The safety factor is therefore computed from the relative distance of the structure assessment point from the origin to the intercept with the constraint modified failure assessment curve. Table 1 presents non-dimensional crack driving forces in the longitudinal direction (service pressure 70 bar), for three defects considered: central semi-spherical crack-like defect with depth $d = t/2$; central semi-elliptical defect of length L ($d = t/2$, $d/L = 0.1$); and central long blunt notch of notch radius ρ ($d = t/2$, $d/L = 0.1$, $\rho = 0.15$ mm), Fig. 7.

Table 1. Non-dimensional crack driving forces in the longitudinal direction with 70 bar as the service pressure.

Orientation of defect	Defect type	$k^*_{c,ref}$	$k^*_{c,struct}$
longitudinal direction	semi-spherical (ss)	0.16	0.12
	semi-elliptical (se)	0.18	0.14
	long blunt notch (ln)	0.25	0.19

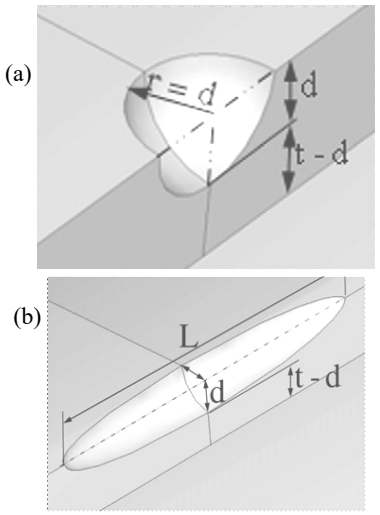

Figure 7. Defect types: (a) central semi-spherical; (b) central semi-elliptical.

The applied notch stress intensity factor is obtained using the volumetric method, /6/. The stress distribution at the notch tip is computed by the finite element method and is extracted from /7/.

The reference fracture toughness is $\delta_{c,0} = 0.54$ mm and the structure fracture toughness $\delta_{c,0} = 0.61$ mm corresponding to a critical effective constraint $\beta_{,c} = 2.1$.

The safety factor, defined as the relative distance from the assessment point to the interception of the loading path with the failure assessment curve is computed for three types of defects. The safety factor relative to the reference failure curve is called $f_{s,T=0,}$ while that relative to the structure failure curve is $f_{s,struct}$. Results are reported in Table 2.

Table 2. Safety factors of three types of defects (ss), (se), (ln); service pressure is 70 bar.

Defect type	$f_{s,T=0}$	$f_{s,struct}$	Difference (%)
(ss)	3.16	3.36	6.4
(se)	3.13	3.29	4.8
(ln)	3.04	3.02	2.8

The use of the constraint modified failure assessment curve provides higher safety factors for the three kinds of defects and gives the possibility of reducing conservatism. The longitudinal long blunt notch shows the most severe defect. In any case, the safety factor is higher than 2, which is considered in the deterministic approach as the required value for safe design.

CONCLUSION

In order to take into account the increase of fracture toughness with the loss of constraint, the failure assessment diagram is modified. It is assumed that the effective stress constraint is proportional to the non-dimensional loading parameter. This assumption introduced into the material failure master curve allows us to know the fracture toughness for any constraint. The considered fracture toughness is therefore introduced to modify the failure assessment curve and the coordinates of the assessment point. These modifications slightly increase the safety factor (by less than 10 %); however, the fracture toughness is increased by 30 % for the specific case described here. The minor increases in the safety factor obtained by using a constraint modified FAD probably do not justify its use.

REFERENCES

1. Pluvinage, G., Ténacite des aciers à basse et moyenne résistance application du critère d'écartement critique de fissuration. Ph.D. Thesis, Lille, 1973. (*Toughness of low- and medium strength steels by applying the criterion of critical crack separation*, in French)
2. Han, K., et al. (2014), *The effect of constraint on CTOD fracture toughness of API X65 steel*, Eng. Fract. Mech., 124-125: 167-181. doi: 10.1016/j.engfracmech.2014.04.014
3. Pluvinage, G., Capelle, J., Hadj Meliani, M. (2014), *A review of fracture toughness transferability with constraint and stress gradient*, Fatig. Fract. Eng. Mater. Struct., 37(11): 1165-1185. doi: 10.1111/ffe.12232
4. American National Standard Institute (ANSI)/American Society of Mechanical Engineers (ASME). Manual for determining strength of corroded pipelines, ASME B31G (1984).
5. Bouledroua, O., Hadj Meliani, M., Pluvinage, G. (2017), *Assessment of pipe defects using a constraint-modified failure assessment diagram*, J Fail. Anal. and Preven., 17(1): 144-153. doi: 10.1007/s11668-016-0221-z
6. Pluvinage, G., Gjonaj, M. (Eds.)., Notch Effects in Fatigue and Fracture, Springer Netherlands, 2001. doi: 10.1007/978-94-010-0880-8
7. Adib-Ramezani, H., Jeong, J., Pluvinage, G. (2006), *Structural integrity evaluation of X52 gas pipes subjected to external corrosion defects using the SINTAP procedure*, Int. J Press. Ves. Piping, 83(6): 420-432. doi: 10.1016/j.ijpvp.2006.02.023

ICSA 2019 – 4th International Conference on Structures and Architecture Lisbon (Portugal), July 24-26, 2019

Aim of the Conference

There is a need to stimulate the inventive and creative design of architectural structures and to persuade architects and structural engineers to collaborate in this process, exploiting together new concepts, applications and challenges.
The aim of ICSA2019 is to present research and developments on the merging of architecture and structural engineering.
Each paper must explore the relation between Structures and Architecture.
The conference will facilitate the meeting of international participants interested in the recent advances in the art, practice and theory of designing and building infrastructures in which the structural and architectonic values are consciously combined and the contribution of each other is mutually enhanced.

Themes

Building envelopes / Facades; Comprehension of complex forms Computer and experimental methods; Concept architectural buildings / Futuristic structures; Concrete and masonry structures Educating architects and structural engineers; Emerging technologies; Glass structures; Innovative architectural and structural design; Lightweight and membrane structures Special structures; Steel and composite structures; Structural design challenges; Tall buildings; The borderline between architecture and structural engineering; History of the relationship between architects and structural engineers; The tectonic of architectural solutions; Use of new materials; Timber structures

Conference Chair

Paulo J. S. Cruz, President of the Intern. Assoc. of Structures and Architecture

Paper Submission

Proceedings will be published by CRC Press / Balkema (Taylor & Francis Group), including a book of extended two-page abstracts and a USB flash card containing the full eight-page papers. These documents are due on November 30, 2018. Acceptance will be notified before February 15, 2019.
Proceedings will be sent for indexation by both Thomson Reuters (Conference Proceedings Citation Index – ISI Proceedings) and Elsevier (Scopus and EI).

Contact Us

ICSA2019 Secretariat, School of Architecture
University of Minho, 4800-058 Guimarães
PORTUGAL
Fax: +351253 510 509
E-mail: secretariat@icsa2019.com
http://www.icsa2019.arquitectura.uminho.pt/